



Cine magnetic resonance urography as a new approach for postoperative evaluation of the reconstructed upper urinary tract: a multicenter study

Xinfei Li*

Zhихua Li*

Xiang Wang

Weijie Zhu

Mingming Ma

Peng Zhang

Hongjian Zhu

He Wang

Xuesong Li

Liqun Zhou

*Xinfei Li and Zhихua Li contribute equally to this paper.

From the Department of Urology (X.L. ✉ lixinfei@pku.edu.cn, Z.L., X.W., W.Z., Xu.L., L.Z.), Peking University First Hospital, Institute of Urology, National Urological Cancer Center, Beijing, China; Department of Radiology, (M.M., H.W.), Peking University First Hospital, Beijing, China; Clinic of Urology (P.Z.), Emergency General Hospital, Beijing, China; Clinic of Urology (H.Z.), Beijing Jiangong Hospital, Beijing, China.

Received 22 April 2021; revision requested 21 May 2021; last revision received 22 November 2021; accepted 09 December 2021.



Epub: 17.01.2023

Publication date: 31.01.2023

DOI: 10.5152/dir.2022.21418

PURPOSE

To evaluate the feasibility and usefulness of cine magnetic resonance urography (cine MRU) as a novel postoperative examination after upper urinary tract reconstruction surgery.

METHODS

Ninety-six patients underwent cine MRU for postoperative evaluation between August 2015 and August 2020. The morphological observations included regular peristalsis, anastomosis, urine flow signals, and reflux. The quantitative evaluations included luminal diameter, peristaltic amplitude, contraction ratio, peristaltic waves, and ureteric jets. The surgical outcomes were classified as success, gray area, or failure by combining the results of cine MRU, symptoms, and the degree of hydronephrosis.

RESULTS

There was no obvious stenosis of the anastomosis in 83 patients (86.46%). Regular peristalsis of the ureter and signals of urination was observed in 85 (88.54%) and 84 patients (87.50%), respectively. In addition, three patients (3.13%) showed urine reflux. The patients in both the success group and the gray area group showed significantly different creatinine levels (success $86.2 \pm 22.3 \mu\text{mol/L}$ vs. failure $110.7 \pm 8.2 \mu\text{mol/L}$, $P = 0.016$; gray area $81.0 \pm 20.0 \mu\text{mol/L}$ vs. failure $110.7 \pm 8.2 \mu\text{mol/L}$, $P = 0.009$) and estimated glomerular filtration rate (success: $88.5 \pm 23.1 \text{ mL/min}\cdot 1.73 \text{ m}^2$, failure: $61.6 \pm 14.1 \text{ mL/min}\cdot 1.73 \text{ m}^2$, $P = 0.014$; gray area: $94.7 \pm 24.6 \text{ mL/min}\cdot 1.73 \text{ m}^2$, failure: $61.6 \pm 14.1 \text{ mL/min}\cdot 1.73 \text{ m}^2$, $P = 0.007$) compared to those in the failure group. The ipsilateral split renal function was 33.6 ± 15.0 , 24.5 ± 13.4 , and $20.1 \pm 0.4 \text{ mL/min}$ in the success, gray area, and failure groups, respectively ($P = 0.354$).

CONCLUSION

Cine MRU demonstrates the morphology and function of the reconstructed upper urinary tract. The results of cine MRU can be used to evaluate the surgical effect, providing guidance for further treatment.

KEYWORDS

Cine MRU, magnetic resonance imaging, reconstructive surgery, ureter, ureteric stricture

Ureteral stenosis can lead to hydronephrosis, recurrent urinary tract infections, or deterioration of renal function. Surgical management mainly focuses on solving the problem of lumen obstruction. However, ineffective peristalsis or no peristalsis of the ureter may still exist after reconstruction surgeries.¹ Moreover, a wide ureter often needs a relatively long time to recover. Because existing follow-up examinations are static assessments, it is difficult to assess the function of the ureter and distinguish between physiological and pathological dilatation.

Cine magnetic resonance imaging (cine MRI), which captures a number of sequential images over a short period of time, enables the dynamic evaluation of an organ's function.² Recent advances in cine MRI techniques allow visualization of peristaltic movement directly and clearly, thus making it a useful tool in the fields of cardiology, obstetrics, gynecology, and gastroenterology.²⁻⁶ Urine is a natural contrast agent, and the ureter anatomy is well visualized by the cine MRI method in T2-weighted images.⁷ However, the role of cine magnetic resonance urography (cine MRU) in the postoperative evaluation of the reconstructed upper urinary tract has not yet been reported. The purpose of the present study is to evaluate the feasibility and usefulness of cine MRU as a novel postoperative examination after upper urinary tract reconstruction surgery.

Methods

Patients

A total of 692 patients underwent surgical treatment for ureteral strictures between August 2015 and August 2020. Out of this number, 96 patients underwent cine MRU for postoperative evaluation. The inclusion criteria included patients who received surgical treatment for ureteral stenosis and volunteered to undergo cine MRU for postoperative evaluation. The exclusion criteria were as follows: (1) no surgery was performed or surgery was intolerable; (2) ureteral stents or nephrostomy tubes had not been removed; (3) patients refused to undergo cine MRU; or (4) patients were unable to cooperate, resulting in failure of the MRU examination or blurred images. Data regarding patient characteristics, symptoms, degree of hydronephrosis, renal function, surgical strategies, and complications were collected. This study was approved by our ethics committee (no: 2020-SR-283) and performed in accordance with the ethical standards of the 1964 Declaration of Helsinki and its subsequent amendments.

Main points

- Cine magnetic resonance urography (cine MRU) displays both the morphology and function of the postoperative upper urinary tract.
- The results of cine MRU can be used to evaluate the surgical effect.
- Cine MRU provides guidance for further treatment in patients who undergo upper urinary tract reconstruction surgery.

Written informed consent was obtained from all patients in the study.

Protocol

All cine MRUs were performed using a 3-T system with a phased-array torso surface coil (Signa Excite TM; GE Medical Systems, Milwaukee, WI, USA). The reconstructed upper urinary tract was identified using a coronal localizer. Static T2-weighted HASTE sequence images, which covered the entire upper urinary tract, were obtained. Using HASTE sequences, the following parameters were applied: field of view = 36 × 36 cm, repetition time = 800 ms, flip angle = 80°, section thickness = 70 mm, matrix = 512, temporal resolution = 0.5 seconds, scan time = 1 second, and time interval = 13 seconds. A series of 30 consecutive specific coronal images was obtained to form a cine loop within a scan time of 407 s.

Image analysis and data sampling

Image analysis was performed by two experienced radiologists using a Picture Archiving and Communication System workstation. Morphological evaluation was performed first by considering the following factors: (1) whether the upper urinary tract was dilated; (2) whether the peristalsis of the reconstructed upper urinary tract was regular and effective; (3) whether the anastomosis was narrow; (4) whether the urine flow signal was unobstructed; and (5) whether reflux existed. Further quantitative measurements taken included luminal diameter, amplitude, contraction ratio, and ureteric jet frequency. When the radiologists had disagreements on morphological evaluation, discussions took place to reach a consensus. For the quantitative measurements, we took an average of the evaluation results as reported by the two radiologists.

Follow up

Patient follow-ups were managed at 1, 3, 6, and 12 months after surgical treatment, then at least once every 6 months. The patients regularly received symptom evaluation, physical examinations, routine urine tests, blood tests [including serum creatinine, estimated glomerular filtration rate (eGFR), electrolytes, and blood gas analysis only for the ileal ureter], and ultrasound at each visit. Cine MRU, renal scintigraphy, and diuretic renograms were performed 3–6 months after the surgery. Surgical success was defined as relief of symptoms and improved/stable hydronephrosis.

Statistical analysis

The surgical outcomes were classified into three categories as follows: success (unobstructed anastomosis and regular peristalsis in cine MRU, relieved symptoms, and improved/stable hydronephrosis), gray area (abnormalities in cine MRU but relief of symptoms, and improved/stable hydronephrosis), and failure (abnormalities in cine MRU, no relief of symptoms, and deteriorated hydronephrosis). All analyses were performed using SPSS Statistics version 24.0 (IBM Corporation). Normally distributed continuous variables were presented by mean ± standard deviation, non-normally distributed continuous variables were presented by median (minimum to maximum), and categorical variables were presented by frequency and percentage. The Kolmogorov–Smirnov test was used to check whether variables had normal distribution. The frequency of categorical variables was compared using chi-square tests. The Fisher–Freeman–Halton test was used when there was a problem with expected count. Differences among the three subgroups were analyzed by either One-Way analysis of variance for normally distributed variables or a Kruskal–Wallis test for non-normally distributed variables, and statistical significance was further subjected to Bonferroni post-hoc analysis. Positive coincidence rate, negative coincidence rate, and Cohen's κ coefficient were calculated to evaluate the concordance of morphological evaluation between the two radiologists. A weighted κ value was used if more than two raters were considered. To analyze the reliability of the normally distributed continuous variables, the intraclass correlation coefficient (ICC) was calculated with the Two-Way random, absolute agreement, and single measures method. Linear regression analysis using the enter method was used to examine the effects of age, body mass index, preoperative creatinine, luminal diameter, peristaltic amplitude, and ureteric jet frequency on postoperative split renal function. A two-sided $P < 0.050$ was considered statistically significant.

Results

A total of 96 patients completed cine MRU after upper urinary tract reconstruction, and the mean age of the patients was 38.0 ± 13.8 years. The reconstructive strategies included ileal ureter (n = 38, 39.58%), pyeloplasty (n = 21, 21.88%), ureteroneocystostomy (n = 9, 9.38%), Boari flap (n = 7, 7.29%), balloon dilation (n = 6, 6.25%), lingual mucosal ureteroplasty (n = 5, 5.21%), appendiceal uret-

eroplasty (n = 3, 3.13%), endoureterotomy (n = 4, 4.17%), ureteroureterostomy (n = 1, 1.04%), ureterolysis (n = 1, 1.04%), and kidney autotransplantation (n = 1, 1.04%). The characteristics and comparisons in the success, gray, and failure groups are shown in Table 1.

Figure 1 shows the cine MRU imaging of the reconstructed upper urinary tract after different surgical strategies (see Supplementary Videos 1-10 for the video results). The positive coincidence rate, negative coincidence rate, and the Cohen's κ coefficient values are shown in Table 2 for the evaluation of anastomotic stenosis, regular peristalsis, ureteral jet, and reflux. The ICC of diameter and amplitude were 0.999 [95% confidence interval (CI) (0.615–1.000), $P < 0.001$] and 0.996 [95% CI (0.898–0.999), $P < 0.001$], respectively. The weighted κ value of the frequency of ureteral jets was 0.958 [95% CI (0.923–0.992), $P < 0.001$]. There was no obvious stenosis

of the anastomosis in 83 patients (86.46%). Regular peristalsis of the ureter and urination signals were observed in 85 (88.54%) and 84 patients (87.50%), respectively. In addition, three patients (3.13%) had urine reflux when asked to urinate. The specific parameters of cine MRU according to different surgical strategies are shown in Supplementary Table 1. Linear regression analysis showed that diameter ($P = 0.153$), amplitude ($P = 0.565$), and frequency of ureteric jet ($P = 0.220$) cannot predict the postoperative split renal function (Table 3 and Supplementary Table 2).

The patients in both the success and gray area groups showed significantly different creatinine levels (success: $86.2 \pm 22.3 \mu\text{mol/L}$ vs. failure: $110.7 \pm 8.2 \mu\text{mol/L}$, $P = 0.016$; gray area $81.0 \pm 20.0 \mu\text{mol/L}$ vs. failure: $110.7 \pm 8.2 \mu\text{mol/L}$, $P = 0.009$) and eGFR (success $88.5 \pm 23.1 \text{ mL/min}\cdot 1.73 \text{ m}^2$ vs. failure: $61.6 \pm 14.1 \text{ mL/min}\cdot 1.73 \text{ m}^2$, $P = 0.014$; gray area: $94.7 \pm 24.6 \text{ mL/min}\cdot 1.73 \text{ m}^2$ vs. failure: $61.6 \pm$

$14.1 \text{ mL/min}\cdot 1.73 \text{ m}^2$, $P = 0.007$) compared to those in the failure group. The ipsilateral split renal function was 33.6 ± 15.0 , 24.5 ± 13.4 , and $20.1 \pm 0.4 \text{ mL/min}$ in the success, gray area, and failure groups respectively, without significant differences ($P = 0.354$) (Table 4).

Discussion

The transportation of urine depends on the peristalsis of the ureter and hydrostatic pressure of the upper urinary tract.⁸ Some pathological conditions have been highlighted as interfering with ureter contraction and triggering dysfunction.¹ Since the effects of long-term hydrostatic expansion and surgical operations on the smooth muscle of the ureter cannot be ignored, postoperative evaluation for the reconstructed upper urinary tract should provide more information to clarify the entire urination process.⁹

Table 1. Baseline characteristics of patients and comparisons in different groups

	Success	Gray area	Failure	P value
n	83 (86.46%)	8 (8.33%)	5 (5.21%)	
Gender				1.000
Male	39 (46.99%)	4 (50.00%)	2 (40.00%)	
Female	44 (53.01%)	4 (50.00%)	3 (60.00%)	
Age (years)	38.0 ± 13.4	36.5 ± 21.4	40.2 ± 6.6	0.897
BMI (kg/m ²)	22.8 ± 4.4	20.6 ± 3.0	24.0 ± 2.9	0.391
Side				0.336
Left	40 (48.19%)	3 (37.50%)	1 (20.00%)	
Right	34 (40.96%)	4 (50.00%)	2 (40.00%)	
Bilateral	9 (10.84%)	1 (12.50%)	2 (40.00%)	
Location				-
Upper	37 (44.58%)	2 (25.00%)	2 (40.00%)	
Middle	9 (10.84%)	0 (0%)	2 (40.00%)	
Lower	31 (37.35%)	6 (75.00%)	1 (20.00%)	
Multiple	1 (1.20%)	0 (0%)	0 (0%)	
Unknown	5 (6.02%)	0 (0%)	0 (0%)	
Stricture length (cm)	$8.5 (0.5-30.0)$	$1.1 (1.0-5.0)$	$10.0 (5.0-21.0)$	0.081
Symptoms				-
Flank pain	31 (37.35%)	2 (25.00%)	1 (20.00%)	
Fever	7 (8.43%)	0 (0%)	0 (0%)	
Nausea or vomit	3 (3.61%)	2 (25.00%)	1 (20.00%)	
Hematuria	4 (4.82%)	0 (0%)	0 (0%)	
Abdominal pain	4 (4.82%)	0 (0%)	0 (0%)	
Anasarca	1 (1.20%)	0 (0%)	0 (0%)	
Asymptomatic	33 (39.76%)	4 (50.00%)	3 (60.00%)	
Preoperative creatinine ($\mu\text{mol/L}$)	81.8 ± 25.6	92.9 ± 47.9	108.5 ± 22.4	0.079
Preoperative ipsilateral split renal function (mL/min)	32.1 ± 17.1	43.0 ± 15.6	30.0 ± 15.6	0.663

BMI, body mass index.

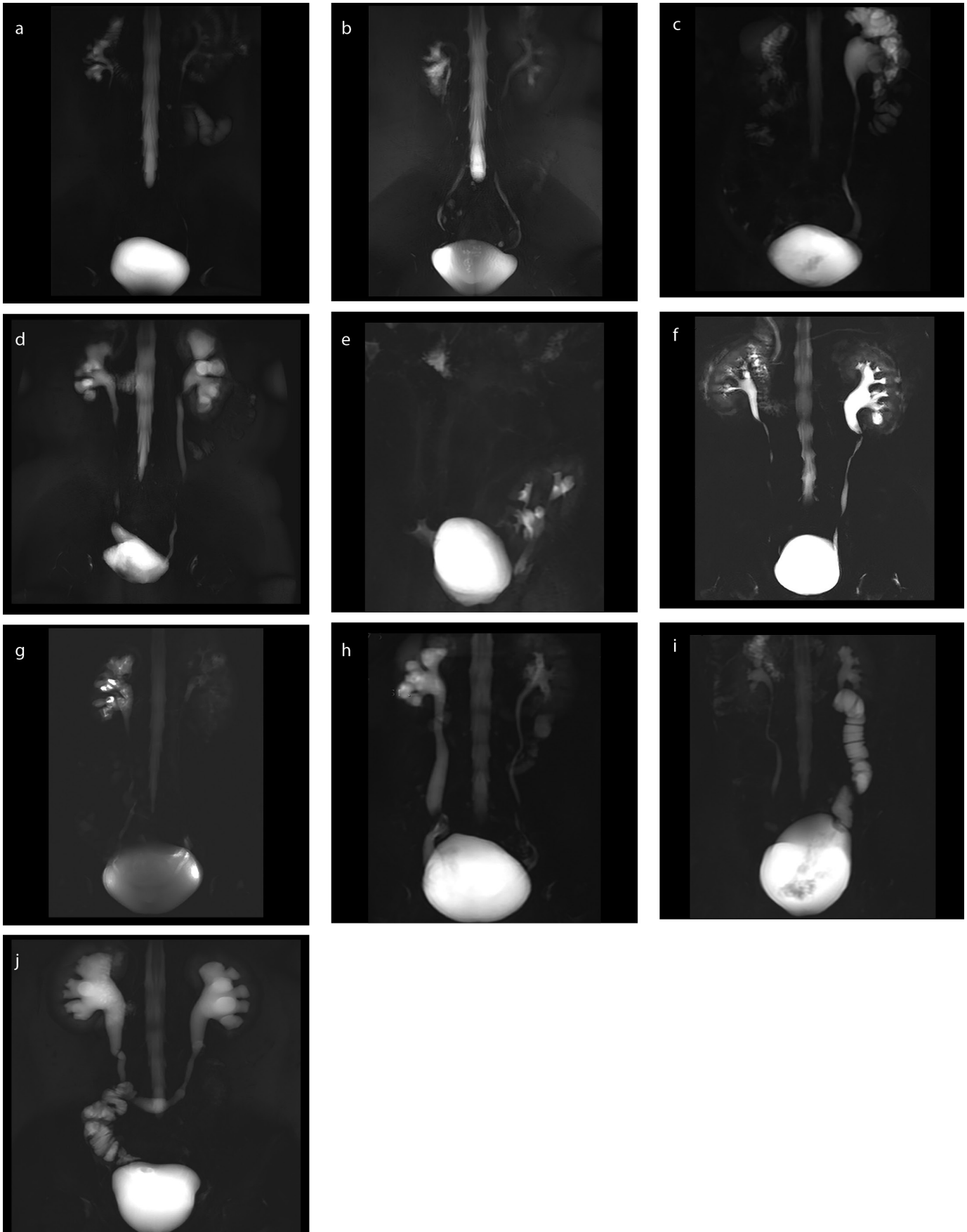


Figure 1. Cine magnetic resonance urography imaging of reconstructed upper urinary tract after different surgical strategies. (a) Ureteroureostomy, (b) ureteroneocystostomy, (c) pyeloplasty, (d) Boari flap, (e) kidney autotransplantation, (f) lingual mucosa graft ureteroplasty, (g) appendiceal ureteroplasty, (h) megaureter, (i) ileal ureter, (j) bilateral ileal ureter

Table 2. Consistency analysis of the morphological evaluation in cine magnetic resonance urography between two radiologists

	Positive coincidence rate	Negative coincidence rate	κ value	<i>P</i> value
Anastomotic stenosis	0.988	0.923	0.911	<0.001
Regular peristalsis	1.000	0.909	0.947	<0.001
Ureteral jet	1.000	1.000	1.000	<0.001
Reflux	1.000	1.000	1.000	<0.001

Table 3. Linear regression analysis of postoperative ipsilateral split renal function

	β	95% CI	Adjusted R square	<i>P</i> value*
Age (years)	-0.274	-0.653–0.105	0.035	0.151
BMI (kg/m ²)	-0.770	-2.110–0.570	0.004	0.248
Preoperative creatinine (μ mol/L)	-0.195	-0.373–0.018	0.112	0.032
Diameter (mm)	-0.641	-1.537–0.255	0.045	0.153
Amplitude (mm)	-0.209	-0.932–0.513	0.005	0.565
Jet	1.635	-1.040–4.310	0.021	0.220

*The *P* values of the regression model and the coefficient are the same for simple linear regression. β , unstandardized regression coefficient; CI, confidence interval; BMI, body mass index.

Table 4. The postoperative creatinine, eGFR, and split renal function in the success, gray area, and failure groups

	Creatinine (μ mol/L)	eGFR (mL/min·1.73 m ²)	Ipsilateral split renal function (mL/min)
Success	86.2 ± 22.3	88.5 ± 23.1	33.6 ± 15.0
Gray	81.0 ± 20.0	94.7 ± 24.6	24.5 ± 13.4
Failure	110.7 ± 8.2	61.6 ± 14.1	20.1 ± 0.4
<i>P</i> value			
Overall	0.016	0.007	0.354
Success vs. failure	0.016	0.014	-
Gray vs. failure	0.009	0.007	-
Success vs. gray	0.613	0.564	-

eGFR, estimated glomerular filtration rate.

The diameter of the normal ureter is 1–6 mm.^{10,11} In our study, the average diameter of the ureter lumen after the operation was larger than normal. The reconstructed upper urinary tract often fails to fully return to normal. However, we found that diameter and peristaltic amplitude were not significantly correlated with postoperative renal function as long as the anastomosis was not narrowed. Routine postoperative examinations only evaluate the degree of upper urinary tract dilatation and do not truly reflect the patient's recovery.¹² Therefore, it is necessary to consider the morphology and quantitative information of the dilated reconstructive upper urinary tract.

Cine MRU provides high-contrast-resolution images with detailed information to demonstrate the general morphology of the postoperative upper urinary tract, including not only peristalsis but also the presence of fixed stenoses.¹³ Dynamic images showed that ureteral stenosis disappeared and that

urine could pass smoothly in a small portion of patients who had suspected anastomotic stenosis, which may have been due to pseudolumen stenosis caused by postoperative inflammation and thickening of the wall. In addition, our results showed that the fixed stenosis had an impact on the recovery of postoperative renal function. Therefore, stenosis captured by cine MRU images requires further treatment to protect renal function.

A previous study has confirmed that urine flow and ureteric jets could be visualized in cine MRU as low-signal waves.¹³ Observation of the urine jet is strong evidence that the reconstructed upper urinary tract is capable of transporting urine, and it is also prevents complete ureteral obstruction.^{14,15} Moreover, the ureteric jet is affected by the diameter and contraction of the ureter.¹⁶ The frequency of ureteric jets also changed accordingly. For unilateral ureteral surgery, the ureteric jets of the contralateral ureter can be used as a reference.

The definition of successful reconstruction in previous studies mainly relied on the relief of symptoms and the relief of obstruction, as is shown in images.¹⁷ Tseng et al.¹⁸ evaluated the success of ureteral reconstruction, where they reduced overestimation of the success rate by a trifecta outcome, which was defined as reserved renal function, no progression of hydronephrosis, and no long-term stent placement. However, the evaluation criteria were relatively subjective.

In the present study, surgical outcomes were divided into success, gray area, and failure categories, combining the results of cine MRU, symptoms, and the degree of hydronephrosis. The creatinine levels and eGFRs of patients were significantly worse in the failure group compared to the success and gray area groups. The split renal function gradually decreased in the success, gray area, and failure groups, but there were no statistically significant differences. We considered that the sample size was not large

enough to reach significant results. Therefore, we proposed that patients in the failure group should receive surgical treatment again to save ipsilateral renal function, while those in the gray area should receive active surveillance, which helps identify abnormalities and determine subsequent strategies. Regular follow-up was sufficient for patients who were evaluated as having a successful outcome.

For the upper urinary tract without hydronephrosis, cine MRU is not recommended for postoperative follow-up. The ureter is long, tortuous, and has a thin lumen. Compared to the heart and uterus, the target is smaller and the variation is greater.¹⁹ It is not easy to obtain a complete upper urinary tract image in the coronal position. In this study, patients with an unclear or not developed ureter had symptom relief and normal renal function during follow-up. Therefore, we recommend using the ultrasound results as the basis for further performance of cine MRU.

There were some limitations to our study. First, the index evaluation of cine MRU needed to be done manually. It is difficult to avoid visual differences between different observers. In addition, the quantitative method of analysis was time-consuming. Second, it is important to determine the quantitative criteria to further standardize the evaluation of cine MRU.²⁰ Third, the quantitative measurement of urine flow and velocity would help in further understanding the upper urinary tract urination function. At present, it has been reported that four-dimensional flow MR is useful in the cardiovascular field,²¹ and additional studies should focus on this issue. Finally, the patients included in this study had different severities of preoperative hydronephrosis and different treatment modalities were adopted, which may lead to bias. Therefore, larger sample sizes are needed in the future.

In conclusion, cine MRU allows for an innovative view of the excretion process of urine. Dynamic images demonstrate the morphology and function of the postoperative upper urinary tract. The results of cine MRU can be used to evaluate the surgical effect by classi-

fying surgical results into success, gray area, or failure categories, thereby providing guidance for further treatment. For non-dilated ureters, the effect of cine MRU is poor.

Conflict of interest disclosure

The authors declared no conflicts of interest.

References

- Whitaker RH. Some observations and theories on the wide ureter and hydronephrosis. *Br J Urol.* 1975;47(4):377-385. [\[CrossRef\]](#)
- Soares DM, Junior HW, Bittencourt LK, Lopes FPPL, de Oliveira MAP. The role of cine MR imaging in the assessment of uterine function. *Arch Gynecol Obstet.* 2019;300(3):545-553. [\[CrossRef\]](#)
- Curtis AD, Cheng HM. Primer and historical review on rapid cardiac CINE MRI. *J Magn Reson Imaging.* 2022;55(2):373-388. [\[CrossRef\]](#)
- Liu S, Zhang Q, Yin C, et al. Optimized approach to cine MRI of uterine peristalsis. *J Magn Reson Imaging.* 2016;44(6):1397-1404. [\[CrossRef\]](#)
- Hoad C, Clarke C, Marciani L, Graves MJ, Corsetti M. Will MRI of gastrointestinal function parallel the clinical success of cine cardiac MRI? *Br J Radiol.* 2019;92(1093):20180433. [\[CrossRef\]](#)
- de Jonge CS, Smout AJPM, Nederveen AJ, Stoker J. Evaluation of gastrointestinal motility with MRI: advances, challenges and opportunities. *Neurogastroenterol Motil.* 2018;30(1). [\[CrossRef\]](#)
- Abreu-Gomez J, Udare A, Shanbhogue KP, Schieda N. Update on MR urography (MRU): technique and clinical applications. *Abdom Radiol (NY).* 2019;44(12):3800-3810. [\[CrossRef\]](#)
- Vahidi B, Fatouree N. A numerical simulation of peristaltic motion in the ureter using fluid structure interactions. *Annu Int Conf IEEE Eng Med Biol Soc.* 2007;2007:1168-1171. [\[CrossRef\]](#)
- Osman F, Romics I, Nyirady P, Monos E, Nádasy GL. Ureteral motility. *Acta Physiol Hung.* 2009;96(4):407-426. [\[CrossRef\]](#)
- Zelenko N, Coll D, Rosenfeld AT, Smith RC. Normal ureter size on unenhanced helical CT. *AJR Am J Roentgenol.* 2004;182(4):1039-1041. [\[CrossRef\]](#)

- Potentia SE, D'Agostino R, Sternberg KM, Tatsumi K, Perusse K. CT Urography for Evaluation of the Ureter. *Radiographics.* 2015;35(3):709-726. [\[CrossRef\]](#)
- Farrugia MK, Whitaker RH. The search for the definition, etiology, and effective diagnosis of upper urinary tract obstruction: the Whitaker test then and now. *J Pediatr Urol.* 2019;15(1):18-26. [\[CrossRef\]](#)
- Zhu WJ, Ma MM, Zheng MM, et al. Cine magnetic resonance urography for postoperative evaluation of reconstructive urinary tract after ileal ureter substitution: initial experience. *Clin Radiol.* 2020;75(6):480.e1-480.e9. [\[CrossRef\]](#)
- de Bessa J Jr, Dénes FT, Chammas MC, et al. Diagnostic accuracy of color Doppler sonographic study of the ureteric jets in evaluation of hydronephrosis. *J Pediatr Urol.* 2008;4(2):113-117. [\[CrossRef\]](#)
- Lojindarat S, Suwikrom S, Puangsa-art S. Postoperative color Doppler sonography of the ureteral jets to detect ureteral patency in laparoscopic hysterectomy. *J Med Assoc Thai.* 2011;94(10):1169-1174. [\[CrossRef\]](#)
- Cvitković Kuzmić A, Brkljčić B, Rados M, Galesić K. Doppler visualization of ureteric jets in unilateral hydronephrosis in children and adolescents. *Eur J Radiol.* 2001;39(3):209-214. [\[CrossRef\]](#)
- Lee M, Lee Z, Koster H, et al. Intermediate-term outcomes after robotic ureteral reconstruction for long-segment (≥ 4 centimeters) strictures in the proximal ureter: a multi-institutional experience. *Investig Clin Urol.* 2021;62(1):65-71. [\[CrossRef\]](#)
- Tseng CS, Tai TE, Hong CH, et al. Trifecta outcome of ureteral reconstruction in iatrogenic injury and non-iatrogenic ureteral lesions: a 10-year experience at a tertiary referral center. *World J Urol.* 2019;37(9):1949-1957. [\[CrossRef\]](#)
- Motola JA, Shahon RS, Smith AD. Anatomy of the ureter. *Urol Clin North Am.* 1988;15(3):295-299. [\[CrossRef\]](#)
- Reiter U, Reiter C, Kräuter C, Nizhnikava V, Fuchsjaeger MH, Reiter G. Quantitative clinical cardiac magnetic resonance imaging. *Rofo.* 2020;192(3):246-256. [\[CrossRef\]](#)
- Azarine A, Garçon P, Stansal A, et al. Four-dimensional Flow MRI: principles and cardiovascular applications. *Radiographics.* 2019;39(3):632-648. [\[CrossRef\]](#)

Supplementary Video 1. Cine magnetic resonance urography imaging after ureterouretostomy

<https://www.youtube.com/shorts/oPRtOb-aJdY>

Supplementary Video 2. Cine magnetic resonance urography imaging after ureteroneocystostomy

<https://www.youtube.com/shorts/xWGUvFDfo0>

Supplementary Video 3. Cine magnetic resonance urography imaging after pyeloplasty

<https://www.youtube.com/shorts/udUPge8w2nQ>

Supplementary Video 4. Cine magnetic resonance urography imaging after Boari flap

<https://www.youtube.com/shorts/GcaSR-DmHys>

Supplementary Video 5. Cine magnetic resonance urography imaging after kidney autotransplantation

<https://www.youtube.com/shorts/MYWhO5oihJs>

Supplementary Video 6. Cine magnetic resonance urography imaging after lingual mucosa graft ureteroplasty

<https://www.youtube.com/shorts/ueQl1XyT9Y4>

Supplementary Video 7. Cine magnetic resonance urography imaging after appendiceal ureteroplasty

<https://www.youtube.com/shorts/PklIzrLPNa4>

Supplementary Video 8. Cine magnetic resonance urography imaging after megaureter

<https://www.youtube.com/shorts/etjvoPvj5YQ>

Supplementary Video 9. Cine magnetic resonance urography imaging after ileal ureter

<https://www.youtube.com/shorts/ImMePNKj2A>

Supplementary Video 10. Cine magnetic resonance urography imaging after bilateral ileal ureter

https://www.youtube.com/shorts/CxA_Se3fbeY

Supplementary Table 1. Detailed information of morphology and quantification in cine MRU

Surgery	Ureter		Dilation		Calyces	Regular peristalsis	Unobstructed anastomosis	Urine jet	Reflux	Diameter (mm)	Amplitude (mm)	Contraction ratio	Urine jet frequency
	Ureter	Pelvis	Pelvis	Ureter									
Pyeloplasty	-	21 (100%)	21 (100%)	11 (52.38%)	21 (100%)	21 (100%)	17 (80.95%)	0 (0%)	4.18 (1.54–7.69)	3.65 (2.07–4.90)	0.301 (0.161–0.540)	4 (0–11)	
Ureteroureterostomy	0 (0%)	1 (100%)	1 (100%)	1 (100%)	1 (100%)	1 (100%)	1 (100%)	0 (0%)	-	2.00	1.00		
Ureteroneocystostomy	6 (66.67%)	9 (100%)	9 (100%)	8 (88.89%)	9 (100%)	9 (100%)	6 (66.67%)	2 (22.22%)	5.47 (2.74–9.73)	3.94 (3.22–5.74)	0.419 (0.371–0.540)	2 (0–4)	
Boari flap	5 (71.43%)	6 (85.71%)	6 (85.71%)	7 (100%)	5 (71.43%)	5 (71.43%)	7 (100%)	0 (0%)	7.32 (3.34–25.57)	5.44 (4.23–6.37)	0.430 (0.406–0.620)	3.5 (1–5)	
Lingual mucosal graft	0 (0%)	5 (100%)	5 (100%)	4 (80.00%)	5 (100%)	5 (100%)	3 (60.00%)	0 (0%)	5.58 (3.87–6.19)	-	-	2 (0–3)	
Appendiceal graft	3 (100%)	3 (100%)	3 (100%)	3 (100%)	3 (100%)	3 (100%)	3 (100%)	0 (0%)	11.77 (5.90–20.12)	-	-	2 (0–2)	
Megaureter	4 (100%)	4 (100%)	4 (100%)	4 (100%)	2 (50.00%)	2 (50.00%)	3 (75.00%)	0 (0%)	12.5 (10.67–15.13)	5.08 (2.57–5.29)	0.346 (0.238–0.528)	5 (0–6)	
Ileal ureter	12 (31.58%)	38 (100%)	38 (100%)	37 (97.37%)	32 (84.21%)	32 (84.21%)	37 (97.37%)	0 (0%)	17.81 (8.01–29.56)	9.77 (4.87–19.90)	0.628 (0.508–790)	3 (0–7)	
Balloon dilation	3 (50.00%)	6 (100%)	6 (100%)	6 (100%)	4 (66.67%)	4 (66.67%)	5 (83.3%)	1 (100%)	5.59 (4.57–16.37)	-	-	4 (0–6)	
Autologous kidney transplantation	1 (100%)	1 (100%)	1 (100%)	1 (100%)	0 (0%)	0 (0%)	1 (100%)	0 (0%)	7.47	1.24	0.166	4	
Adhesion lysis	0 (0%)	0 (0%)	0 (0%)	1 (100%)	1 (100%)	1 (100%)	1 (100%)	0 (0%)	-	-	-	3	

Cine MRU, cine magnetic resonance urography.

Supplementary Table 2. The linear regression model with postoperative renal function as the dependent variable using entry method

	β	95% CI	P value (coefficient)	adjusted R square	P value (model)
Age (years)	-0.142	-0.743–0.458	0.615		
BMI (kg/m ²)	-0.553	-2.505–1.400	0.549		
Preoperative creatinine (μ mol/L)	-0.195	-0.474–0.085	0.155		
Diameter (mm)	-0.765	-2.963–1.432	0.462	0.005	0.459
Amplitude (mm)	0.762	-3.136–4.659	0.678		
Jet	1.738	-2.053–5.528	0.338		

β , unstandardized regression coefficient; CI, confidence interval; BMI, body mass index.